RESEARCH ARTICLE
doi: 10.2306/scienceasia1513-1874.2007.33.265

*ScienceAsia* 33 (2007): **265-271**

# ATF3 Transgenic Mice: Structural Analysis of Cardiac Myocytes

**Wuthichai Klomkleaw[a*], Prasarn Tangkawattana[b], Tsonwin Hai[c], Yoshichika Okamoto[c], Makoto Muto[d] and Mamoru Yamaguchi[e]**

[a] Department of Veterinary Anatomy, Faculty of Veterinary Science, Chulalongkorn University, Bangkok, Thailand.
[b] Department of Veterinary Anatomy, Faculty of Veterinary Medicine, Khon Kaen University, Khon Kaen, Thailand.
[c] Department of Molecular and Cellular Biochemistry and Center for Molecular Neurobiology, The Ohio State University, Columbus, Ohio, USA.
[d] Department of Veterinary Surgery, School of Veterinary Medicine, Azabu University, Kanagawa, Japan.
[e] Department of Veterinary Biosciences, College of Veterinary Medicine, The Ohio State University, Columbus, Ohio, USA.

* Corresponding author, E-mail: Wuthichai.K@Chula.ac.th

*Received 15 Feb 2006*
*Accepted 9 Jan 2007*

**ABSTRACT:** Over-expression of the activating transcription factor 3 (ATF3) in transgenic (TG) mice induces atrial enlargement. This manuscript reports anatomical and structural alterations in TG mice hearts. A statistical analysis showed that hearts of the TG mice (0.61±0.2 grams) are significantly heavier than those of non-transgenic (nTG) mice (0.16±0.03 grams) ($P<0.05$). The average myocyte cross-sectional area of the TG mice (172.51±72.72 $\mu m^2$) was significantly larger than that of nTG mice (74.4±16.46 $\mu m^2$) ($P<0.05$). The alterations varied greatly among individual atria, with and without visible calcification. Approximately 56% of TG mice produced recognizable calcification in the right atrium. Moreover, very few apoptotic cells were observed. Ultrastructural studies of the enlarged atria showed 1) degeneration and degradation of cytoplasmic components and mineralization of mitochondria leading to total destruction and death of myocytes, 2) hyperchromatic-hypertrophic nuclei with various nuclear inclusions, 3) fibrosis and mineralization of the myocardial layer, and 4) thrombus, cartilage and bone formation. It is possible that cellular injury would cause energy metabolism impairment and/or sarcolemmal malformation leading to $Ca^{++}$ accumulation and subsequent ultrastructural changes. Although pathogenesis of this alteration remains unclear, ATF3 could be involved in these abnormalities.

**KEYWORDS:** ATF3, mice, cardiac myocytes.

## INTRODUCTION

The activating transcription factor 3 (*ATF3*) gene encodes a member of the ATF/cyclic adenosine monophosphate (cAMP)-responsive element-binding protein (ATF/CREB) family of transcription factors. These proteins have a basic region-leucine zipper DNA-binding domain and function as stress-inducible transcriptional repressors[1-5]. Rat ATF3 was shown to have ability to transform primary cultures of chick embryo fibroblasts by promoting growth factor-independent proliferation[6]. ATF3 would possess an intrinsic oncogenic nature by inducing DNA synthesis and expression of cyclin-D1 like in hepatocytes[7]. It was also suggested that ATF3 plays a critical role in accelerating caspase protease activation during DNA damaging agent-induced (camptothecin and etoposide) apoptosis[8].

Cardiophysiological effects of ATF3 were studied in transgenic mice having human *ATF3* over-expression which was generated in the FVB/N background with ATF3 expression under the control of the $\alpha$-myosin heavy chain ($\alpha$-MHC) gene promoter[9]. Quantitative RNA dot-blot analysis showed significant up-regulation of mRNA levels of markers for cardiac hypertrophy, such as $\alpha$-skeletal actin, atrial natriuretic factor and $\beta$-MHC in transgenic mice hearts[9]. Several interesting characteristics including biatrial enlargement were obtained through echocardiography[9]. The alteration of myocytes in the myocardial layer directly affects the function of the atrium and induces various diseases. The over-expression of *ATF3* apparently targets the atrium and induces destruction and degradation of cytoplasm[9]. In this manuscript, we further examined several structural alterations of the enlarged atria.

## MATERIALS AND METHODS

### Sample sources

Ten *ATF3* over-expressing transgenic (TG) and fifteen non-transgenic (nTG) control mice with FVB/N background of both sexes, 2-50 weeks of age, were

obtained from Neurobiotechnology Center, Department of Molecular and Cellular Biochemistry, The Ohio State University, USA. At the age of 2, 4, 6, 12, 19, 20, 21, 29, 32 and 50 weeks old, the animals were randomly picked, weighed and then sacrificed by decapitation. After washing and flushing out excess blood with 50 mM PBS, hearts were dissected out with minimal stumps of aorta, cranial vena cava and caudal vena cava remaining and then weighed.

### Histological and ultrastructural study

Samples for light microscopy were processed according to routine procedures. Terminal uridine nick end labeling (TUNEL) staining was accomplished using ApopTag® (Intergen, Purchase, NY) to reveal apoptosis. Staining was done following the manufacture's instruction. The samples were observed with a Zeiss photomicroscope III.

Thin sections (~80nm) were cut on an ultramicrotome using a diamond knife and stained with 1% uranyl acetate followed by Reynold's lead citrate. The samples were evaluated with a transmission electron microscope (Hitachi H-300) at accelerating voltage of 75 kV.

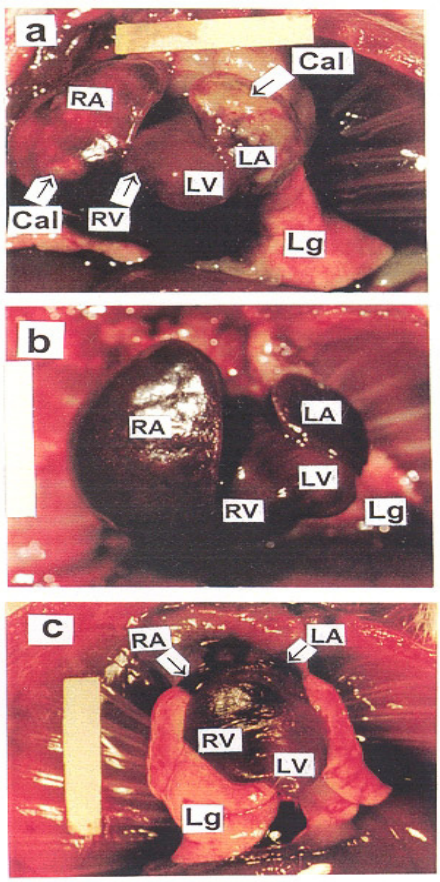


**Fig 1.** Hearts of ATF3 transgenic (a,b) and nontransgenic control mice (c) were compared. Atrial enlargement and calcification (Cal) is noticeable in TG mice. RA: right atrium; RV: right ventricle; LA: left atrium; Lg: lung; LV: left ventricle. Bar (horizontal in a, vertical in b and c) = 1 cm.

### Measurement of atrial myocyte cross-sectional area

A total of 1,370 atrial myocyte cross-sectional areas from both TG (733 areas) and nTG mice (637 areas) of various ages (2-50 weeks) were measured mainly at the nuclear level. The measurement was performed on pictures taken under a Zeiss Photomicroscope III light microscope with a digital camera (INSIGHT®) using SPOT® software (Diagnostic Instruments, Sterling Heights, MI).

### Statistical analysis

Paired Student's t-tests were performed to evaluate the mean differences of body weight, heart weight and atrial myocyte size between the two animal groups. The analyses were performed with Windows® SPSS (version 11.0).

## Results

In general, size of the heart of TG mice appeared comparatively larger than that in nTG mice (Fig 1). At the age of 2 weeks, the right atrium of a TG mouse appeared to be slightly larger than the left atrium. In older mice, atrial enlargement was obvious in hearts of TG mice compared with those of nTG mice. The size of each atrium increased by more than 1 centimeter, with the right atrium being slightly larger than the left and even larger than the length of ventricles (Fig 1a, b). Multifocal calcification of the atrial walls was visible in about 56% of the TG mice with dilated atria (Fig 1a) in comparison with the nTG mouse (Fig 1c). However, calcification was not found in some of the TG mice hearts with enlarged atria (Fig 1b). No apparent gross anatomical changes were observed in the left ventricle (LV) and right ventricle (RV) of the TG hearts at any age.

Average heart weight of the TG mice (0.61±0.2 grams) was significantly higher than that of the nTG mice (0.16±0.03 grams) ($P<0.05$). The average atrial myocyte cross-sectional area of the TG mice heart increased more rapidly than in the nTG mice when increasing age (Table 1). Myocyte cross-sectional area was approximately two times larger in the TG mice than in the nTG mice younger than 10 weeks old, and the difference increased to a factor of three in mice older than 30 weeks. The average areas varied from 70 $\mu m^2$ in the 4-week-old TG mice to 305.1 $\mu m^2$ in the 32-week-old TG mice, with an overall average of 173±73 $\mu m^2$. These areas were significantly much larger than those in the nTG groups which ranged from 50.05 $\mu m^2$ in the 4-week-old nTG mouse, to 96.09 $\mu m^2$ in the 12-week-

old nTG mouse with an overall average of 74±16 μm² (P<0.05).

**Table 1.** Showing number of myocytes counted and average cross-sectional areas in each age group. TG: transgenic, nTG: non-transgenic.

| Age (weeks) | TG mice | | nTG mice | |
|---|---|---|---|---|
| | # of myocytes counted | Average area (μm²) | # of myocytes counted | Average area (μm²) |
| 2 | 35 | 100.40 | 70 | 70.10 |
| 4 | 58 | 70.03 | 38 | 50.05 |
| 6 | 111 | 182.30 | 62 | 70.00 |
| 12 | 95 | 195.16 | 69 | 96.09 |
| 19 | 69 | 145.20 | 46 | 60.04 |
| 20 | 36 | 140.28 | 28 | 52.61 |
| 22 | 29 | 138.59 | 98 | 81.75 |
| 29 | 130 | 171.75 | 34 | 84.24 |
| 32 | 114 | 305.10 | 17 | 85.56 |
| 50 | 56 | 276.27 | 175 | 93.92 |
| **Average** | 73 ±35 | 173 ±73 | 64 ±46 | 74 ±16 |

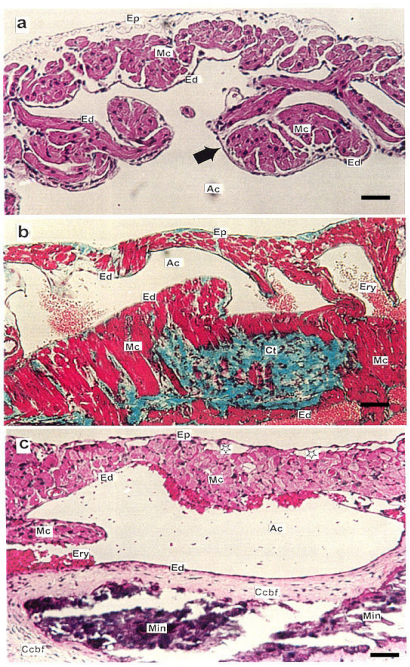


**Fig 2.** H&E (a,c) and trichrome (b) staining sections from comparable areas show general views in the development of calcification (Min) in the atria of TG (b,c) and nTG mice (a).
a) Distribution of myocytes in the myocardium (Mc) shows a distinct papillar-pleated pattern (arrow).
b) Substantial accumulation of connective tissue (Ct) within myocardium (Mc).
c) Dilated vacuolar spaces (star) in the epicardial area is often filled with blood.
Ac: atrial chamber; Ccbf: circular collagen bundles with fibroblasts; Ed: endocardium; Ep:epicardium; Ery: Erythrocytes. Bar = 30 μm (a-c).

TG Heart is composed of fibroblasts and randomly oriented collagen fibers with scattered mineral deposition. The three basic structural layers of the TG mice hearts (epicardium, myocardium and endocardium) were altered with myocyte degeneration, connective tissues increment, circular collagen bundles with fibroblasts formation, dilated vascular spaces, and mineralization (calcification) and bone formation (Fig 2b-c, Fig 3a-b). The myocardial layer lost most of its myocytes and was replaced entirely by connective tissue and minerals, as shown in Fig 3a. Advanced mineralization results in formation of bone enclosing an area with bone marrow containing various progenitor blood cells (Fig 3b, inset). Myocyte degeneration and hypertrophy could often be observed together with extensive cytoplasmic component degradation, vacuolization and hyperchromatic-hypertrophic nuclei (Fig 4). Few nuclei showed TUNEL-positive staining (Fig 5a, ApN), indicating that lower degree of apoptosis was present. One rare apoptotic nucleus with disappearance of nuclear membrane captured under the electron microscope clearly indicated that the myocyte was undergoing karyolysis (Fig 5b). In an advanced stage, atrial myocytes were extremely irregular in size and shape, and some nuclei (Fig 4a, c-d) became much larger than those in a normal mouse (Fig 4b, inset) and sometimes became

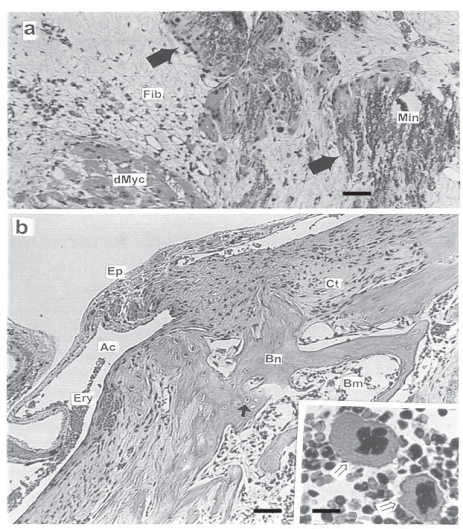


**Fig 3.** TG mice atrium stained with H&E. Ac: atrial chamber; Bm: bone marrow; Ep: epicardium; Ery: erythrocytes.
a) Mineralization (bone formation) (Min) in the myocardium is shown in later stages of atrial alteration. Fibrosis network (Fib) is abundant with diminishing in number of myocyte (arrows). Bar = 30 μm.
b) Bone spicules (Bn) with osteocytes (arrow) in association with connective tissue (Ct) in myocardial area are shown. In the inset, two megakaryocytes (open arrows) are observed in bone marrow. Bar = 30 μm (b), 7.5 μm (inset).

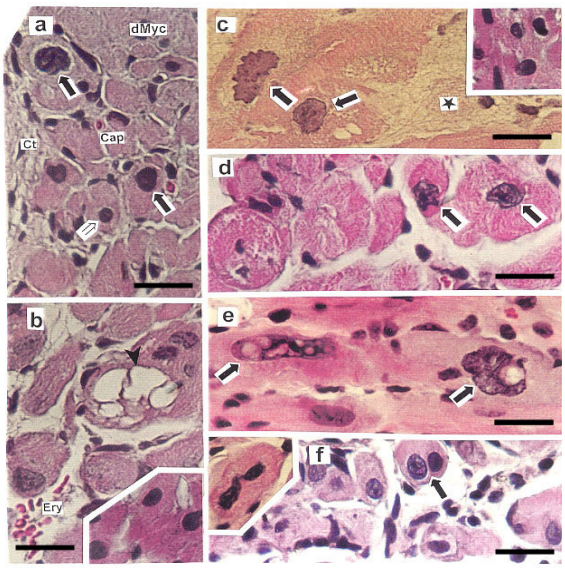


**Fig 4.** H&E staining samples showing progression of atrial myocyte alteration. Cap: Capillaries; Ery: erythrocytes. Bar = 15 μm (a-f)

a) Both normal (open arrow) and degenerated myocytes (dMyc) with hyperchromatic and hypertrophic nuclei (dark arrow) are shown. Intercellular connective tissue (Ct) increases with the presence of dMyc.

b) Cytoplasmic vacuolization often occurs (arrowhead). Normal myocytes of nTG mouse is shown in inset.

c) Degraded myocytes (star) with semi-degraded cytoplasm and irregularly shaped nuclei (arrows) in comparison with normal nuclei (inset).

d) The hyperchromatic and hypertrophic nuclei (arrows) appear within hypertrophic myocytes.

e) Intranuclear vacuolizations with hypertrophy (arrows) are also seen in a TG mouse.

f) Binucleated myocytes can also be observed (arrow). An elongated nucleus with bending indicates cell division in a 29-week-old TG mouse (inset).

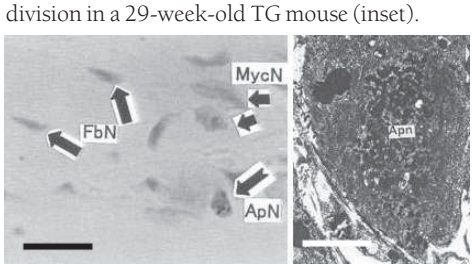


**Fig 5.** Light and electron micrographs showing myocardial apoptosis in a TG mouse left atrium.

a) A TUNEL peroxidase with methyl green counterstained sample shows several positive-staining atrial myocyte nuclei (arrows). The number of observed apoptotic nuclei (ApN) is low, suggesting that cytoplasmic digestion and destruction are responsible for most of the cell death. MycN: normal myocyte nuclei; Fbn: fibroblast nuclei. Bar = 15 μm.

b) An apoptotic nucleus (Apn). Bar = 1.3 μm.

binucleated (Fig 4f). Although there were no specific structural patterns or characteristics of myocyte alteration with age, older mice seemed to have more myocyte destruction, which was finally replaced by bony tissue.

The fine structure of altered myocytes was further revealed by electron microscopic observation (Fig 6-8). The destruction of myocytes included degradation of myofibrils and myofilaments, streaming, breakage and disappearance of Z-lines, degeneration of mitochondria, accumulation of glycogen particles and destruction of intercalated discs (Fig 6). In fig 6, most of the cytoplasmic components in Myc1 and Myc5 were destroyed, whereas some myofibril remnants were still visible in Myc2, Myc3 and Myc4. Various degrees of myocyte destruction can also be seen in Fig 6 inset 2. Non membranous laminar formed nuclear inclusions (lam) can be clearly distinguished from cytoplasmic inclusions (Fig 7a, c). The crystalline-like Golgi complex (Fig 7b) can be observed in addition to the abnormal appearance of the Golgi complex. TG mouse mitochondria appeared to be much smaller compared to the mitochondria in normal muscle (Fig 8a). The deposition of minerals, presumed to be mainly $Ca^{++}$ salts, started initially with the appearance of mosaic

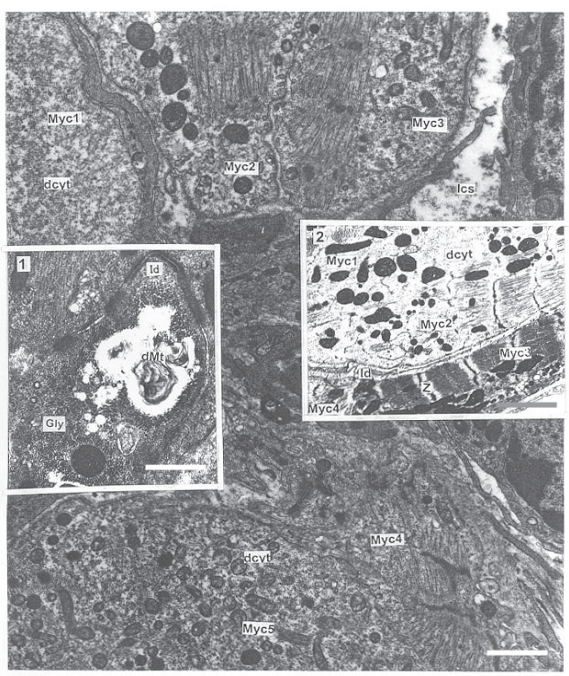


**Fig 6.** Electron micrograph showing many myocytes (Myc1–Myc5) with degenerated cytoplasmic materials (dcyt) of the right atrium of a TG mouse. An enlargement of these materials is in inset 2. Typical glycogen (Gly) accumulation in association with a digested mitochondrial vacuole (dMt) is observed near the intercalated disc (Id) (inset 1). Ics: intercellular space. Bar = 0.78 μm, 0.67 μm (inset 1), 2 μm (inset 2).

structure (Fig 8b, arrows). Mitochondria further developed mineral deposition or aggregates to form vacuolization with and without residues of digested aggregates (Fig 8b-d). Mineralization of the myocardial layer extends to the intercellular spaces together with collagen fiber accumulation (Fig 8d, arrow and inset). In contrast, no such structural transformation was observed in atria of nTG mice at any age.

## Discussion

The biatrial enlargement seen in the TG mice should be a sequel of pathological hypertrophy (i.e., eccentric hypertrophy or dilated cardiomyopathy) in association with destruction of myocytes and their components[16] rather than physiological hypertrophy, which is evidenced by the increase of muscle mass, normal myofilaments and other cytoplasmic organelles. Both sexes of mice have been used in this study as explained in the Materials and Methods. There have been several studies that reported that there are sex differences in the electrophysiological properties[17], ventricular depolarization[18], emergence of ischaemic preconditioning and ischaemia-reperfusion of the mouse heart[19]. However, there was no evidence about influence of sex on size of the heart and cardiac myocytes for the FVB/N strain used in this study.

In addition, the extremely low number of apoptotic nuclei suggests that cytoplasmic digestion and destruction is responsible for most of the cell death rather than apoptosis. The pathology would probably be the result of earlier or higher expression of the *ATF3* in the atria than the ventricles[10-13]. Cellular injury would be initiated by proteases which could be activated by the ATF3[8]. Although we did not examine intracellular calcium content, it is possible that the initial cellular injury would further trigger energy metabolism impairment or sarcolemmal alteration leading to an

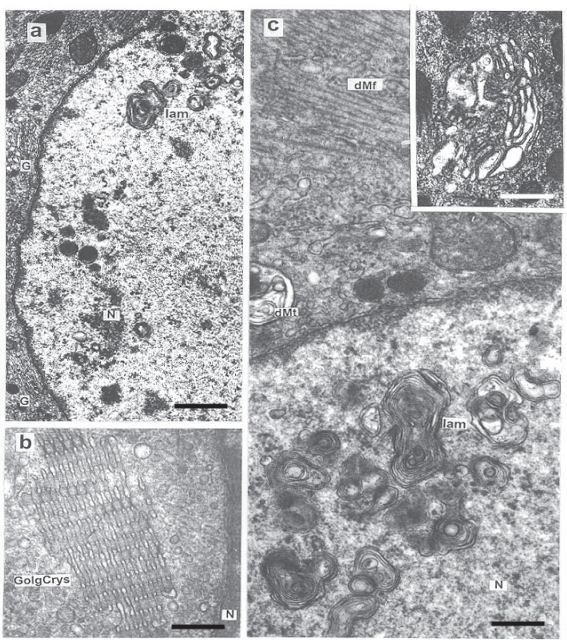


**Fig 7.** Electron micrographs of atrial myocytes of a TG mouse.
a) Lamellated inclusions (lam) in nucleus (N) are shown. Bar = 0.67 μm
b) Golgi apparatus occasionally appears in Golgi crystals (GolgCrys). Bar = 0.3 μm
c) A nucleus containing lamellated inclusion (Iam) surrounded by partially degraded myofibrils (dMf), a degenerated mitochondrial vacuole (dMt) is shown. Abnormal feature of Golgi apparatus at juxtaposition to nuclear membrane is also found (inset). Bar = 0.75 μm, 0.27 μm (inset).

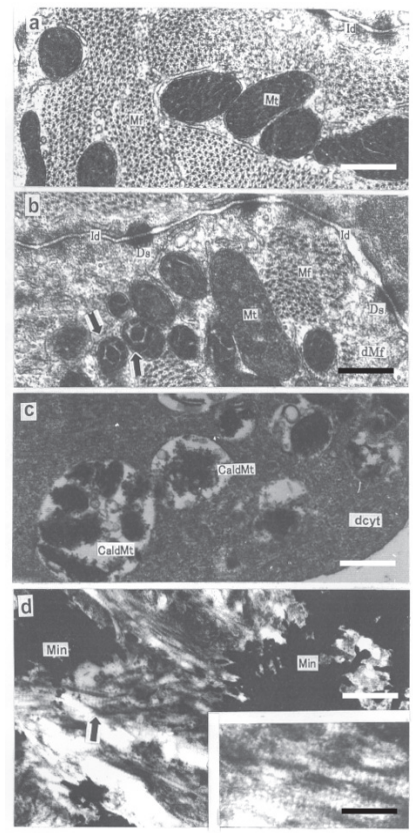


**Fig 8.** Electron micrographs of the left atrium (a-c) and left ventricle (d) of a TG mouse showing:
a) Normal mitochondrial (Mt);
b) Mitochondria with a dense mosaic structure (arrows) suggesting deposition of some minerals in their cristae;
c) Mitochondria with mineral deposition and vacuolization (CaldMt);
d) Typical mineralization (Min) among collagen fibers (arrow; inset).
dcyt: digested cytoplasm; dMf: digested myofibrils; Ds: desmosomes; Id: intercalated disc; Mf: myofibrils. Bar = 0.27 μm (a,b), 0.4 μm (c), 0.75 μm (d) and 0.43 μm (d, inset).

elevation of the intracellular $Ca^{++}$ concentration[20]. Accordingly, the elevated calcium would increase the activity of proteolytic enzymes causing extensive cytoskeletal destruction, cell shape alteration and activation of phospholipases. The cell would finally undergo membrane damage and mitochondrial calcification[20]. Calcification in mitochondria would probably be the starting point of mineral accumulation that allows intracellular deposition of insoluble calcium phosphate, as has been reported in freeze-thaw injury of mouse hearts[21]. Connective tissue stroma surrounding mineralized areas was followed eventually by calcification.

The fast-growing and abnormal expansion of the myocardium of the atrial wall, along with the ventricular diastolic load to the atria, could cause the disruption of the endocardium. With exposure to blood turbulence in the chamber and accumulation of blood cells, platelets, fibrin and macrophages, this site could be a nidus for mural fibrin thrombosis. The thrombi became larger and more organized with fibroblast infiltration, especially in the peripheral area. These fibroblasts could differentiate to chondroblasts and chondrocytes, which then form cartilage[22,23]. Osteoblasts, believed to be derived from bone marrow stromal cells[28], traveled through the blood circulation to replace the chondrocytes and form bone. Then, hematopoietic bone marrow was produced in the area of pathological ossification[12]. Chondrification and ossification in the vascular thrombi of these mice were similar to other reports[24-27].

Either macroscopic or microscopic calcification would occur in response to the ATF3 expression regardless of the nature of the animal strain and age, since it was observed only in the TG mice but not in the non-transgenic control mice. However, there is evidence that suggests that myocardial calcification is normal for the some strains of mice, for example, DBA/2[14]. Furthermore, a diet low in magnesium and high in phosphorus can also cause severe calcification of the heart[15].

The intranuclear inclusions observed under the electron microscope could be simply identified through their electron-dense membrane. Since the inclusion has the same membrane density as the nucleus or is composed of single membrane, it is most likely formed within nucleus and can be considered as true inclusion. The crystalline-like Golgi complex is extremely interesting; however, more advanced techniques may be needed to identify this material.

In conclusion, over-expression of the *ATF3* gene induced atrial hypertrophy in mice. The effects of the over-expressed protein varied greatly in individual mouse atria, with and without macroscopically recognizable calcification. However, all hypertrophic myocytes exhibited various cytoplasmic and nuclear component alterations. The replacement of myocytes with connective tissue in the myocardial layer accelerated destruction of the atrial wall. An increase in dilated vascular space, mineral deposition, chondrocyte deposition, cartilage formation and bone formation occurred in myocardial layer. The formation of cartilagenous thrombi in the atrial chambers accelerates destruction of the entire heart. Thus far, pathogenesis of atrial phenotypes especially to explain why TG right atria were often much larger than the left atria remains an open question.

## Acknowledgements

We thank Erika Cochrane Seeler for statistical analysis and critical comments on the manuscript. We also thank Dr. Steven Weisbrode and Dr. Geraldine Fuller for the helpful discussions. This work was supported in part by grants from the American Heart Association and Muscular Dystrophy Association (M.Y.) and DK59605 (T.H.).

## References

1. Cai Y, Zhang C, Nawa T, Aso T, Tanaka M, Oshiro S, Ichijo H, and Kitajima S (2000) Homocysteine-responsive ATF3 gene expression in human vascular endothelial cells: Activation of c-Jun NH2-terminal kinase and promoter response element. *Blood* **96**, 2140-8.
2. Hai T, Wolfgang CD, Marsee DK, Allen AE, and Sivaprasad U (1999) ATF3 and stress responses. *Gene Expres* **7**, 321-35.
3. Hai T and Hartman MG (2001) The molecular biology and nomenclature of the activating transcription factor / cAMP responsive element binding family of transcription factors: Activating transcription factor proteins and homeostasis. *Gene* **273**, 1-11.
4. Sassone-Corsi P (1994) Goals for signal transduction pathways: linking up with transcriptional regulation. *EMBO* 13, 4717-28.
5. Ziff EB (1990) Transcription factors: a new family gathers at the cAMP response site. *Trends Genet* **6**, 69-72.
6. Perez S, Vial E, van Dam H, and Castellazzi M (2001) Transcription factor ATF3 partially transforms chick embryo fibroblasts by promoting growth factor-independent proliferation. *Oncogene* **20**, 1135-41.
7. Allan AL, Albanese C, Pestell RG, and LaMarre J (2001) Activating transcription factor 3 induces DNA synthesis and expression of cyclin D1 in hepatocytes. *J Biol Chem* **276**, 27272-80.
8. Mashima T, Udagawa S, and Tsuruo T (2001) Involvement of transcriptional repressor ATF3 in acceleration of caspase protease activation during DNA damaging agent-induced apoptosis. *J Biol Chem* **188**, 352-8.
9. Okamoto Y, Chaves A, Chen J, Kelley R, Jones K, Weed HG, Gardner KL, Gangi L, Yamaguchi M, Klomkleaw W, Nakayama T, Hamlin RL, Carnes C, Altschuld R, Bauer J, and Hai T (2001) Transgenic mice with cardiac-specific expression of activating transcription factor 3, a stress-inducible gene, have conduction abnormalities and contractile dysfunction. *Am J Pathol* **159**, 639-50.

10. de Groot IJ, Lamers WH, and Moorman AF (1989) Isomyosin expression pattern during rat heart morphogenesis: an immunohistochemical study. *Anat Rec* **224**, 365-73.
11. Subramaniam A, Jones WK, Gulick J, Wert S, Neumann J, and Robbins J (1991) Tissue-specific regulation of the alpha-myosin heavy chain gene promoter in transgenic mice. *J Biol Chem* **266**, 24613-20.
12. Jones WK, Sanchez A, and Robbins J (1994) Murine pulmonary myocardium: developmental analysis of cardiac gene expression. *Dev Dyn* **200**, 117-28.
13. Palermo J, Gulick J, Colbert M, Fewell J, Robbins J (1996) Transgenic remodeling of the contractile apparatus in the mammalian heart. *Circulation Res* **78**, 504-9.
14. Kruppenbacher JP, Arnold G, Mertens T, Fischer A, Zimmermann J, and Eggers HJ (1993) Outbred mice infected by an encephalomyocarditis virus variant: a model for studying chronic viral heart disease. *Virchows Arch A Pathol Anat Histopathol* **422**, 405-13.
15. van den Broek FA and Beynen AC (1998) The influence of dietary phosphorus and magnesium concentrations on the calcium content of heart and kidneys of DBA/2 and NMRI mice. *Lab Anim* **32**, 483-91.
16. Hoshijima M, Pashmforoush M, Knoll R, and Chien K R (2002) The MLP family of cytoskeletal Z disc protein and dilated cardiomyopathy: A stress pathway model for heart failure progression. *Cold Spring Harbor Symposia on Quantitative Biology* **67**, 399-408.
17. Larsen JA and Kadish AH (1998) Effects of gender on cardiac arrhythmias. *J Cardiovas Electrophysiol* **9**, 655-64.
18. Abi-Gerges N, Philp K, Pollard C, Wakefield I, Hammond TG and Valentin JP (2004) Sex differences in ventricular repolarization: from cardiac electrophysiology to Torsades de Pointes. *Fundament Clin Pharmacol* **18**, 139-51.
19. Song X, Li G, Vaage J and Valen G (2003) Effects of sex, gonadectomy, and oestrogen substitution on ischaemic preconditioning and ischaemia-reperfusion injury in mice. *Acta Physiol Scand* **177**, 459-66.
20. Trump BF, Berezesky IK, Laiho KU, Osornio AR, Mergner WJ, and Smith MW (1980) The role of calcium in cell injury. A review. *Scan Electron Microsc* 492, 437-62.
21. Russell JW, Biller J, Hajduczok ZD, Jones MP, Kerber RE, and Adams HP Jr (1991) Ischemic cerebrovascular complications and risk factors in idiopathic hypertrophic subaortic stenosis. *Stroke* **22**, 1143-7.
22. Blazer VS and Gratzek JB (1985) Cartilage proliferation in response to metacercarial infections of fish gills. *J Comp Pathol* **95**, 273-80.
23. Hoshi K, Amizuka N, Sakou T, Kurokawa T, and Ozawa H (1997) Fibroblasts of spinal ligaments pathologically differentiate into chondrocytes induced by recombinant human bone morphogenetic protein-2: morphological examinations for ossification of spinal ligaments. *Bone* **21**, 155-62.
24. Aoyagi S, Nishimi M, Hiratsuka R, Takaseya T, and Teshima H (2001) Right atrial thrombus associated with combined valvular disease: case report. *J Heart Valve Dis* **10**, 542-4.
25. Spencer K, Weinert L, and Pentz WH (1999) Calcified right atrial mass in a woman receiving long-term intravenous phosphate therapy. *J Am Soc Echocardiogr* **12**, 215-7.
26. Minatoya K, Okabayashi H, Yokota T, and Hoover EL (1996) Calcified ball thrombus in the left atrium. *Ann Thorac Surg* **61**, 1513-4.
27. Salyer WR and Salyer DC (1975) Myxoma-like features of organizing thrombi in arteries and veins. *Arch Pathol* **99**:307-11.
28. Siddiqi A, Parsons MP, Lewis JL, Monson JP, Williams GR, and Burrin JM (2002) TR expression and function in human bone marrow stromal and osteoblast-like cells. *J Clin Endocrinol Metab* **87**, 906-14.